

# Small-angle X-ray solution scattering study on the dimerization of the FKBP25mem from *Legionella pneumophila*

Bettina Schmidt<sup>a</sup>, Stephan König<sup>b</sup>, Dmitri Svergun<sup>c,\*\*</sup>, Vladimir Volkov<sup>c,\*\*</sup>, Gunter Fischer<sup>a,\*</sup>, Michel H.J. Koch<sup>c</sup>

<sup>a</sup>Max-Planck-Gesellschaft, Arbeitsgruppe 'Enzymologie der Peptidbindung', Weinbergweg 16a, D-06120 Halle/Saale, Germany

<sup>b</sup>Institut für Biochemie, Abteilung Enzymologie, Martin-Luther-Universität Halle-Wittenberg, Weinbergweg 16a, D-06099 Halle/Saale, Germany

<sup>c</sup>European Molecular Biology Laboratory, EMBL, c/o DESY, Notkestraße 85, D-22603 Hamburg, Germany

Received 12 June 1995; revised version received 10 August 1995

**Abstract** The dimerization of the FK506-binding peptidyl-prolyl *cis/trans*-isomerase (PPIase) FKBP25mem (Mip (macrophage infectivity potentiator) protein) from *Legionella pneumophila* was studied by small-angle X-ray solution scattering. A value of 44 kDa, independent on the protein concentration between 2 and 13 mg/ml, confirming that FKBP25mem is a dimer was found for the molecular mass of the protein. The radius of gyration of the protein is 3.3 nm and the Porod volume 87 nm<sup>3</sup>. A model of the shape of FKBP25mem was evaluated from the scattering curve. Each monomer consists of a proximal and a peripheral domain, which are perpendicular to each other. The envelope of the crystallographic model of human FKBP12 fits well into the peripheral domain. The contact regions between the two monomers in the dimeric protein are probably located between the N-terminal parts of the monomers.

**Key words:** Small-angle X-ray solution scattering; FKBP25mem; *Legionella pneumophila*; Dimer; Peptidyl-prolyl *cis/trans*-Isomerase; Spherical harmonics

## 1. Introduction

The enzyme class of peptidyl-prolyl *cis/trans*-isomerases (PPIases; EC 5.2.1.8) consists presently of four families, the cyclophilins (CyPs), FK506-binding proteins (FKBPs), parvulins, and trigger factors, having only little, if any, sequence similarity with each other. They catalyse the *cis/trans*-isomerization of peptidyl-prolyl bonds in oligopeptides and accelerate slow rate-limiting steps in the refolding of proteins in vitro and in vivo (for a review, see [1,2]). This catalytic activity is inhibited by their tight binding to the immunosuppressive drugs cyclosporin A or FK506 and rapamycin. Cyclophilins and FKBPs occur in mammals as well as plants, fungi and bacteria, but until now an PPIase-active member of the parvulin family was only found in *Escherichia coli* [3,4].

Several proteins in different organisms and cell types were found to be associated with cyclophilins or FKBPs. The human host cell protein cyclophilin18 binds specifically to a four proline stretch of the HIV-1 Gag polypeptide and the presence of Cyp18 in the virus particle was shown to be essential for the

infectivity of the virions [5,6]. Cyclophilins as well as FKBPs are assembled into inactive steroid receptor complexes. Human FKBP52 and the homologous mouse (p59), rabbit (FKBP59) and chicken proteins (hsp56) are immunophilins binding the heat-shock proteins hsp90 and hsp70 and are components of the unliganded glucocorticoid or progesterone receptor complex [7–12]. PPIase activity inhibited by FK506 in the nmol range was determined for FKBP51 purified from Jurkat cells [9], for recombinant human FKBP52 [7], and for glutathion-S-transferase-fusion proteins of full-length rabbit FKBP59 (HBI) and its two N-terminal domains [11]. Information about the enzymatic activity of the proteins within the steroid receptor complexes is, however, lacking. Besides their ability to form heterooligomeric complexes with heat-shock proteins and steroid receptors homooligomerization was observed for a 17,000 fragment, resulting from limited digestion of chicken thymus FKBP52, and for the Jurkat cell FKBP51 only in the presence of FK506 [9,10]. Radanyi et al. [13] examined rabbit FKBP59-HBI in non-denaturing polyacrylamide gel electrophoresis, density gradient and gel filtration analysis giving no suggestion for homooligomerization of the native protein which is not complexed with FK506. In contrast to that we were recently able to show that FKBP25mem (Mip protein) from the Gram-negative bacterium *Legionella pneumophila*, the causative agent of Legionnaires' disease, is active as a homodimer with the monomeric form having little, if any, PPIase activity compared to the dimeric enzyme [14]. The protein is located at the outer membrane surface of the cells and was shown to be one major virulence factor of this organism. FKBP25mem-negative mutants have reduced ability to survive in their eukaryotic host cells, macrophages and monocytes [15,16]. The PPIase activity of *L. pneumophila* FKBP25mem is inhibited by FK506 in the nmol range and the substrate specificity profile toward synthetic peptides is similar to that of human (h) FKBP12 [17].

Amino acid sequence analysis of *L. pneumophila* FKBP25mem revealed the existence of two domains in the primary structure. The N-terminal sequence (residues 1–106 of the mature protein) has no similarity to any known protein except Mip homologues. The C-terminal part of the protein shows high homology to FKBPs with the conservation of 10/14 residues of hFKBP12 located within a 4-Å surrounding from the bound ligand FK506 [18].

The 3-D structure of FKBP12 was extensively studied with and without bound ligands in solution and in crystals (for a review, see [19]). Both the structure determination by NMR and X-ray crystallography showed that FKBP12 is composed by a five-stranded  $\beta$ -sheet which wraps around a short amphiphilic

\*Corresponding author. Max-Planck-Gesellschaft, Arbeitsgruppe 'Enzymologie der Peptidbindung', Weinbergweg 16a, D-06120 Halle/Saale, Germany. Fax: (49) (345) 5511972.

\*\*On leave from the Institute of Crystallography, Russian Academy of Science, Leninsky Prospekt 59, 117333 Moscow, Russian Federation.

$\alpha$ -helix. The hydrophobic binding site for FK506 is located between the  $\alpha$ -helix and the interior wall of the  $\beta$ -sheet [18,20,21]. According to secondary structure prediction, the C-terminal part of FKBP25mem seems to contain the same structural properties as hFKBP12.

In this work, we describe experiments on the self-association behaviour of *L. pneumophila* FKBP25mem using small-angle X-ray solution scattering. It is shown that over a large range of concentration (2–13 mg/ml) the protein exists as a dimer in solution. The shape of FKBP25mem evaluated from the scattering curves using spherical harmonics suggests possible contact regions between the monomers.

## 2. Experimental

### 2.1. Protein purification and sample preparation

The FKBP25mem was purified from the recombinant *E. coli* strain HB101 (pBLL 106) [17] according to Ludwig et al. [22]. The pure protein was concentrated and dialysed against 20 mM Hepes/NaOH buffer, pH 7.0, using a centricon concentrator 10,000 Da (Amicon). Protein concentration was determined spectrophotometrically. Extinction coefficients at 280 nm were calculated from amino acid sequence according to Gill and von Hippel [23]. As shown by measurements of circular dichroism and catalytic activity, the protein was not damaged by irradiation during small-angle X-ray solution scattering experiments.

PPIase activity was determined using the synthetic peptide Suc-Ala-Phe-Pro-Phe-4-nitroanilide as substrate in a 2-step reaction coupled to chymotrypsin developed by Fischer et al. [24] using a Hewlett Packard 8452 diode array UV/VIS spectrophotometer. Secondary structure predictions were made using the HIBIO PROSIS version 7.0 software (Hitachi Software, Brisbane, USA).

### 2.2. X-ray solution scattering

The data were collected on the X33 camera [25–27] of the EMBL on the storage ring DORIS of the Deutsches Elektronen Synchrotron (DESY) using multiwire proportional chambers with delay line readout [28]. Data were collected at two different camera lengths covering ranges of momentum transfer  $s = 4\pi\sin\theta/\lambda$  ( $2\theta$  is the scattering angle and  $\lambda$  the wavelength) between  $0.15 < s < 1.8 \text{ nm}^{-1}$  and  $0.65 < s < 4.0 \text{ nm}^{-1}$ . For the low-angle measurements, solutions with 2–9 mg/ml were used to avoid interparticle interferences whereas for the higher angles the concentrations were up to 20 mg/ml. The data were normalized to the intensity of the incident beam, corrected for the response of the detector, the scattering of the buffer was subtracted and the statistical errors were calculated using the program SAPOKO (Svergun and Koch, unpubl. data). Data from the two different  $s$ -ranges were scaled for concentration and merged by equalizing the mean value of the scattering in the range  $0.65 < s < 1.85 \text{ nm}^{-1}$ .

### 2.3. Methods of data analysis

Preliminary estimate of the maximum particle size was obtained by a method based on orthogonal expansion [29]. The experimental data were then processed using the indirect transform program package GNOM [30–32] to evaluate the particle distance distribution function  $p(r)$ . The shape of the dimeric particle was evaluated by multipole expansion [33–35]. The 3-D density distribution  $\rho(r)$  of a monomer is approximated in spherical coordinates  $(r, \theta, \phi)$  by an angular boundary function  $F(\omega)$  of  $\omega = (\theta, \phi)$  such that  $\rho(r) = 1$  for  $r < F(\omega)$  and  $\rho(r) = 0$  for  $r > F(\omega)$ . This shape function is developed into a series of spherical harmonics  $Y_{lm}(\theta, \phi)$  as:

$$F(\omega) = \sum_{l=0}^L \sum_{m=-l}^l f_{lm} Y_{lm}(\omega) \quad (1)$$

The angular resolution is  $\pi/(L+1)$ , and the coefficients  $f_{lm}$  are complex numbers. The scattering intensity of the monomer is then

$$I_m(s) = 2\pi^2 \sum_{l=0}^L \sum_{m=-l}^l |A_{lm}(s)|^2 \quad (2)$$

where the partial amplitudes  $A_{lm}(s)$  are evaluated from the coefficients  $f_{lm}$  via the power series representation. The amplitudes  $A_{lm}(s)$  enable to evaluate the scattering from a second monomer obtained by the symmetry operation. Assuming for simplicity that the 2-fold axis coincides with the  $z$ -axis, the scattering intensity from the dimer  $I_d(s)$  is the function of the  $f_{lm}$  coefficients of the monomer and the distance  $X$  between the centres of monomers along the  $x$ -axis. These are the unknowns which are evaluated using an adaptive non-linear least-squares fit [36] to the processed experimental intensities (Svergun, Barberato, Volkov and Koch, in prep.).

## 3. Results and discussion

The experimental data from FKBP25mem were first processed with the orthogonal expansion program to give an esti-

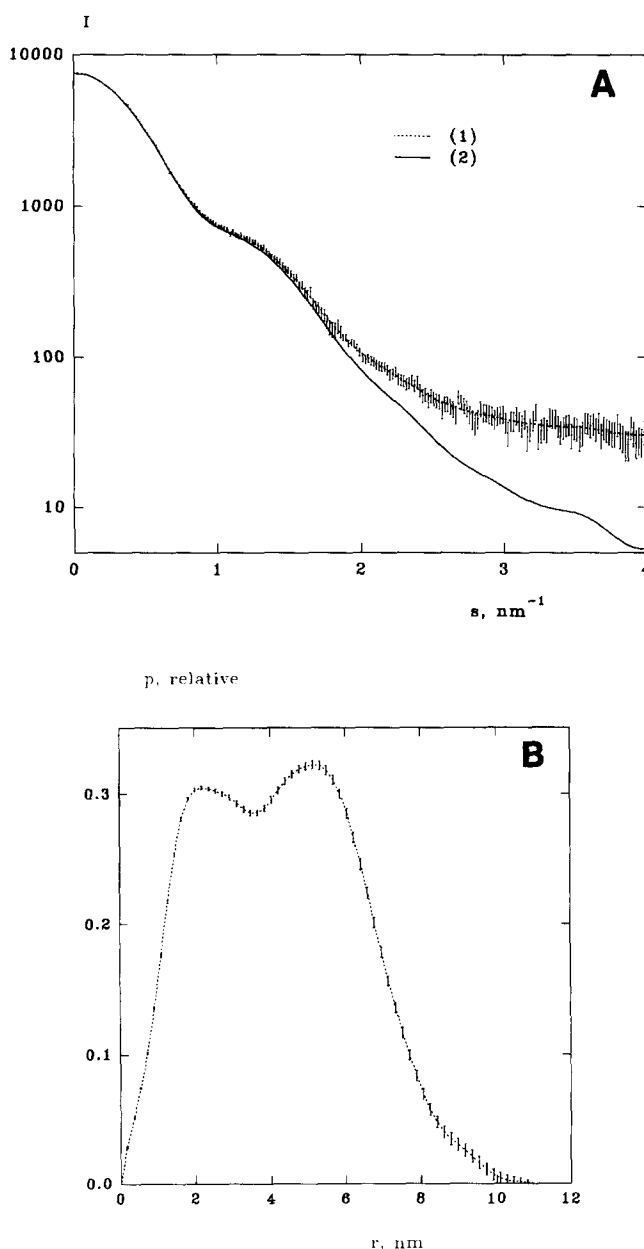


Fig. 1. (a) Experimental curve from FKBP25mem (points with error bars), processed curve (1), the processed curve after subtracting a constant and the scattering from the final model (2); (b) distance distribution function with error bars.

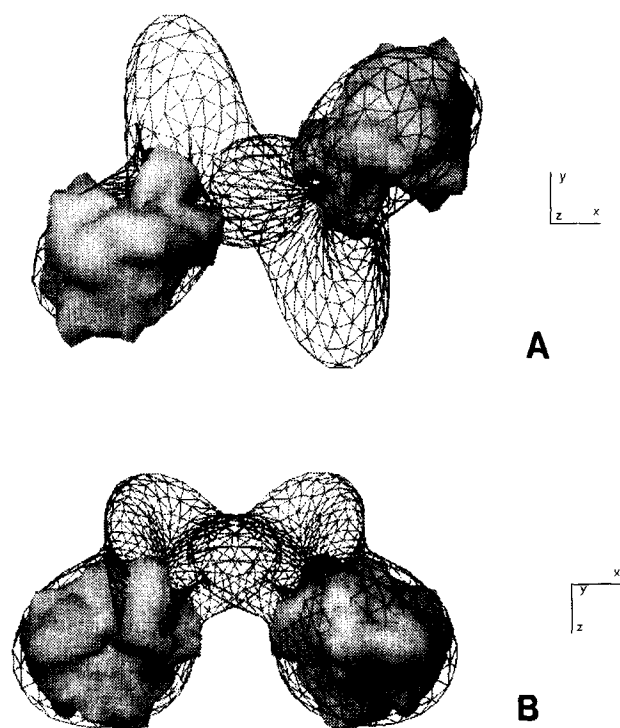


Fig. 2. Model of the dimer of FKBP25mem together with the envelopes of human FKBP12 fitted into the peripheral domains. The two-fold axis coincides with  $z$ -axis, the length of the axes is 2 nm. FKBP25mem is displayed as a wireframe and hFKBP12 as a shaded solid. Fig. b is obtained by rotating Fig. a around  $x$ -axis clockwise by  $90^\circ$ .

mate of the particle maximum diameter  $D = 11$  nm. Results of the data treatment by the indirect program GNOM using this maximum diameter are presented in Fig. 1. The  $p(r)$  function (Fig. 1b) is bimodal suggesting that the particle is a dimer and this is confirmed by the fact that the normalized forward scattering of FKBP25mem (molecular mass 22,800) is  $\sim 5\times$  that of lysozyme (molecular mass 15,000). The particle invariants, radius of gyration ( $R_G = 3.3$  nm) and the Porod volume ( $V = 87$  nm<sup>3</sup>) are also consistent with the dimeric form of FKBP25mem in solution and indicate that the particle is rather anisometric.

The molecular mass calculated from the scattering patterns of the FKBP25mem is 44,000. It is independent on the protein concentration between 2 and 13 mg/ml as indicated by the proportional dependence of the extrapolated forward scattering ( $I_0$ ) on the protein concentration. This is confirmed by the nmol dissociation constant of the dimer determined by kinetic measurements published earlier [14].

For the shape determination of FKBP25mem, the processed curve was normalized to the Porod volume and a constant was subtracted to reduce the influence of the intraparticle inhomogeneities and force the  $s^{-4}$  behaviour at large  $s$ . The resulting curve (Fig. 1a) was then fitted by the minimization algorithm searching for the shape of a monomer and the centre-to-centre distance between the two monomers in the dimer. The resulting shape of FKBP25mem up to the multipole resolution  $L = 4$  corresponding to a spatial resolution of  $\sim 2$  nm is presented in Fig. 2. Differences between the scattering curve from this model and curve 2 in Fig. 1a are not recognizable in the plot. This model is described by  $(L + 1)^2 + 1 = 26$  parameters, out of

which 5 parameters are correlated due to the rotations and the arbitrary displacement of the centre of mass of the monomer along the 2-fold axis. This leaves 21 parameters which are still not entirely independent because of the condition  $F(\omega) > 0$ . The range of measurements contains  $(s_{\max} D_{\max} / \pi) + 1 = 15$  Shannon's channels which gives an estimate of the number of independent parameters in the experimental data set [37,38]. The above considerations justify the use of the model up to the resolution  $L = 4$  but should not be taken as the suggestion that the model is unique. Interpretation of the diffraction data is always ambiguous especially as the correlation between the observed data and the model parameters is non-linear. In fact, starting from different initial approximations, several different models with  $L = 4$  can be generated which produce practically the same scattering curve. They all, however, show similar features, namely that the monomer consists of two well-defined domains, one proximal and one peripheral, which are perpendicular to each other. The model in Fig. 2 has been selected to give the best visual overlap between the two proximal domains, and also the best fit between the shape of the peripheral domain and that of hFKBP12. The models at lower resolution ( $L = 3$ ) also provide a reasonable fit to the experimental data up to  $s = 2$  nm<sup>-1</sup> but fail to follow the trend of the scattering curve at higher momentum transfers. The agreement between the model ( $I_{\text{mod}}$ ) and the experimental data ( $I_{\text{exp}}$ ) measured by the  $R$ -factor defined as:

$$R = \frac{\int_0^{s_{\max}} |I_{\text{exp}}(s) - I_{\text{mod}}(s)| s^2 ds}{\int_0^{s_{\max}} I_{\text{exp}}(s) s^2 ds}$$

in the range  $0 < s < 4$  nm<sup>-1</sup> is  $1.2 \cdot 10^{-2}$  at  $L = 3$  against  $2.1 \cdot 10^{-3}$  at  $L = 4$ .

Primary sequence analysis and secondary structure prediction according to the algorithm of Chou and Fasman [39] and Rose [40] showed that the FKBP25mem consists of two domains. The C-terminal domain exhibits 35% identity and 55% homology, respectively, with the amino acid sequence of hFKBP12. According to secondary structure prediction, this domain has a globular folding similar to that of hFKBP12, including the hydrophobic binding pocket which is also indicated by the similar substrate specificity profiles of the two PPIases measured with synthetic peptides [17,41]. The N-terminal domain (residues 1–106) shows no homology to any known protein and is suggested to contain a long  $\alpha$ -helix, including residues 34–70 [14]. The envelope of the atomic model of hFKBP12 evaluated from the Brookhaven PDB coordinates [42] differs significantly in shape from the proximal domain of the FKBP25mem monomer but can be neatly fitted to the elongated peripheral domain (Fig. 2). The chosen orientation of the hFKBP12 within the peripheral domain allows the elongation of the N-terminal part of the amino acid chain into the proximal, N-terminal domain of the FKBP25mem. The shape model of FKBP25mem dimer gives some ideas for possible contact regions between the monomers, confirming that the dimerization involves mostly the N-terminal domains, especially the long  $\alpha$ -helices, of each monomer, as we suggested earlier [14]. Preliminary experiments with the cloned C-terminal domain of the FKBP25mem showed that this part of the protein alone is inactive as a PPIase, probably due to the stabiliza-

tion of the monomeric state (B. Schmidt, unpubl. data), which also supports the model in Fig. 2.

This model of the shape and the position of the FKBP25mem monomers in the dimeric protein provides now a starting point for further investigations on the role of this activity-related dimerization in mediating virulence of *L. pneumophila*.

**Acknowledgements:** The work was supported by the Bundesministerium für Bildung, Wissenschaft, Forschung und Technologie, Project 055NHLAB7, the International Association for the Promotion of Co-operation with Scientists from the Independent States of the Soviet Union (INTAS) under Contract 93-0645, by NATO Linkage Grant LG 921231 and by the EMBO Fellowship of V. Volkov. We thank Dr. Birgit Ludwig for providing and culture the *E. coli* strain HB101 (pBLL106).

## References

- [1] Schmid, F.X. (1993) Annu. Rev. Biophys. Biomol. Struct. 22, 123–143.
- [2] Schmid, F.X., Mayr, L.M., Mücke, M. and Schönbrunner, E.R. (1993) Adv. Prot. Chem. 44, 25–66.
- [3] Rahfeld, J.U., Schierhorn, A., Mann, K. and Fischer, G. (1994) FEBS Lett. 343, 65–69.
- [4] Rahfeld, J.U., Rücknagel, K.P., Schelbert, B., Ludwig, B., Hacker, J., Mann, K. and Fischer, G. (1994) FEBS Lett. 352, 180–184.
- [5] Rosenwirth, B., Billich, A., Datema, R., Donatsch, P., Hammer-schmid, F., Harrison, R., Hiestand, P., Jaksche, H., Mayer, P., Peichl, P., Quesniaux, V., Schatz, F., Schuurman, H.J., Traber, R., Wenger, R., Wolff, B., Zenke, G. and Zurini, M. (1994) Antimicrob. Agents Chemotherap. 38, 1763–1772.
- [6] Thall, M., Bukovsky, A., Kondo, E., Rosenwirth, B., Walsh, C.T., Sodroski, J. and Göttlinger, H.G. (1994) Nature 372, 363–365.
- [7] Peattie, A.D., Harding, W.M., Fleming, A.M., Decenzo, T.M., Lippke, A.J., Livingston, J.D. and Benasutti, M. (1992) Proc. Natl. Acad. Sci. USA 89, 10974–10978.
- [8] Pratt, W.B., Czar, M.J., Stancato, L.F. and Owens, J.K. (1993) J. Steroid. Biochem. Mol. Biol. 46, 269–279.
- [9] Wiederrecht, G., Hung, S., Chan, K.H., Marcy, A., Martin, M., Calaycay, J., Boulton, D., Sigal, N., Kincaid, L.R. and Siekierka, J.J. (1992) J. Biol. Chem. 267, 21753–21760.
- [10] Yem, A.W., Reardon, I.M., Leone, J.W., Heinrikson, R.L. and Deibel, M.R. (1993) Biochemistry 32, 12571–12576.
- [11] Chambrud, B., Rouvierefourmy, N., Radanyi, C., Hsiao, K., Peattie, D.A., Livingston, D.J. and Baulieu, E.E. (1993) Biochem. Biophys. Res. Commun. 196, 160–166.
- [12] Stancato, L.F., Chow, Y.H., Owensgrillo, J.K., Yem, A.W., Deibel, M.R., Jove, R. and Pratt, W.B. (1994) J. Biol. Chem. 269, 22157–22161.
- [13] Radanyi, C., Chambrud, B. and Baulieu, E.E. (1994) Proc. Natl. Acad. Sci. USA 91, 11197–11201.
- [14] Schmidt, B., Rahfeld, J., Schierhorn, A., Ludwig, B., Hacker, J. and Fischer, G. (1994) FEBS Lett. 352, 185–190.
- [15] Cianciotto, N.P., Eisenstein, B.I., Mody, C.H., Toews, G.B. and Engleberg, N.C. (1989) Infect. Immun. 57, 1255–62.
- [16] Cianciotto, N.P. and Fields, B.S. (1992) Proc. Natl. Acad. Sci. USA 89, 5188–5191.
- [17] Fischer, G., Bang, H., Ludwig, B., Mann, K. and Hacker, J. (1992) Mol. Microbiol. 10, 1375–1383.
- [18] Van Duyne, G.D., Standaert, R.F., Karplus, P.A., Schreiber, S.L. and Clardy, J. (1993) J. Mol. Biol. 229, 105–24.
- [19] Braun, W., Kallen, J., Mikol, V., Walkinshaw, M.D. and Wüthrich, K. (1995) FASEB J. 9, 63–72.
- [20] Michnick, S.W., Rosen, M.K., Wandless, T.J., Karplus, M. and Schreiber, S.L. (1991) Science 252, 836–839.
- [21] Van Duyne, G.D., Standaert, R.F., Karplus, P.A., Schreiber, S.L. and Clardy, J. (1991) Science 252, 839–842.
- [22] Ludwig, B., Rahfeld, J., Schmidt, B., Mann, K., Wintermeyer, E., Fischer, G. and Hacker, J. (1994) FEMS Microbiol. Lett. 118, 23–30.
- [23] Gill, C.S. and von Hippel, H.P. (1989) Anal. Biochem. 182, 319–326.
- [24] Fischer, G., Bang, H. and Mech, C. (1984) Biomed. Biochim. Acta 43, 1101–1111.
- [25] Boulin, C., Kempf, R., Koch, M.H.J. and McLaughlin, S.M. (1986) Nucl. Instrum. Methods A249, 399–407.
- [26] Boulin, C.J., Kempf, R., Gabriel, A. and Koch, M.H.J. (1988) Nucl. Instrum. Methods A269, 312–320.
- [27] Gabriel, A. and Dauvergne, F. (1982) Nucl. Instrum. Methods 201, 223–224.
- [28] Svergun, D.I. (1993) J. Appl. Cryst. 26, 258–267.
- [29] Svergun, D.I., Semenyuk, A.V. and Feigin, L.A. (1988) Acta Cryst. A44, 244–250.
- [30] Svergun, D.I. (1991) J. Appl. Cryst. 24, 485–492.
- [31] Svergun, D.I. (1992) J. Appl. Cryst. 25, 495–503.
- [32] Stuhmann, H.B. (1970a) Acta Cryst. A26, 297–306.
- [33] Stuhmann, H.B. (1970b) Z. Phys. Chem. Frankfurt 72, 177–184, 185–198.
- [34] Svergun, D.I. and Stuhmann, H.B. (1991) Acta Cryst. A47, 736–744.
- [35] Dennis, J., Gay, D. and Welsch, R. (1981) ACM Trans. Math. Soft. 7, 348–368, 369–383.
- [36] Moore, P.B. (1980) J. Appl. Cryst. 13, 168–175.
- [37] Taupin, D. and Luzzati, V. (1982) J. Appl. Cryst. 15, 289–300.
- [38] Chou, P.Y. and Fasman, G.D. (1978) Annu. Rev. Biochem. 47, 251–276.
- [39] Rose, G.D. (1978) Nature 272, 586–590.
- [40] Harrison, R.K. and Stein, R.L. (1990) Biochemistry 29, 3813–6.
- [41] Svergun, D.I., Barberato, C. and Koch, M.H.J. (1995) J. Appl. Cryst. (in press).